Journal of Aerosol Science 106 (2017) 1–10

Contents lists available at ScienceDirect

Journal of Aerosol Science

journal homepage: www.elsevier.com/locate/jaerosci

Contact electrification in aerosolized monodispersed silica microspheres quantified using laser based velocimetry

Stefano Alois[a,b,*], Jonathan Merrison[a], Jens Jacob Iversen[a], Jörn Sesterhenn[b]

[a] Instutute of Physics and Astronomy, Aarhus University, Ny Munkegade 120, building 1520, 8000 Aarhus C, Denmark
[b] Institute of Fluid Mechanics and Engineering Acoustics, Technische Universität Berlin, Müller-Breslau-Str. 15, 10623 Berlin, Germany

ARTICLE INFO

Keywords:
Contact electrification
Microspheres
Solid aerosol
Laser Velocimetry

ABSTRACT

The contact electrification of aerosolized micro particles has been studied using a novel technique involving laser velocimetry. This has allowed the simultaneous determination of size and electrical charge of individual silica microspheres (in the range 1 – 8 μm). Interestingly the particles interacting with the injector tube have been seen to become electrified with a relatively narrow range of surface charge concentration of around $Q/4\pi r^2 \sim -100\ e^-/\mu m^2$ (~ -0.02 mC/m^2) for all particle sizes. Several combinations of aerosol particle and injector tube composition were also investigated, some of which led to positive particle electrification and all of which resulted in similar values of measured surface charge concentration. The electrification was not seen to be strongly affected by gas composition and is in reasonable agreement with the expected maximum surface charge observed in previous experiments (< 0.1 mC/m^2). Possible explanations for this effect are discussed, including the possibility of field emission at the contact site. In the future this technique is intended also to be applied to particle-particle induced contact electrification and its material dependence.

1. Introduction

Contact electrification (tribo-electrification) is an important physical process in the transport of fine solid materials (i.e. micrometer scale) and especially in the generation and dynamics of solid particle aerosols, examples are in Aeolian transport, volcanoes, atmospherics, pharmaceuticals etc. (Harrison et al., 2016; James et al., 2008; Karner & Anne Urbanetz, 2011; Merrison, 2012). Despite the importance of contact electrification and the amount of research in this field, there is little agreement upon the mechanism of charge transfer. Generally it is now thought that there are several competing processes occurring and not one single mechanism responsible and that this is dependent upon the nature of the interacting surfaces and especially the surface chemistry. On the most fundamental level one may consider contact electrification to occur via charge exchange with the transfer of electrons and/or ions, material transfer is considered to be a form of ion transfer (Tanoue, Ema, & Masuda, 1999). There are several models involving each of these processes which have been successfully applied in respective experimental cases. A complete picture for all materials in all cases still eludes researchers and has been a source of active debate for decades (Harper, 1998; Harrison et al., 2016; Lowell & Rose-Innes, 1980; McCarty & Whitesides, 2008).

For non-ionic insulators (e.g. polymers and possibly including mineral sand/dust) most researchers attempt to employ electron exchange models (Lowell & Rose-Innes, 1980; Matsusaka, Maruyama, Matsuyama, & Ghadiri, 2010). However contact electrification does not seem to correlate with surface or bulk electron properties such as dielectric constant, atomic properties,

* Corresponding author at: Instutute of Physics and Astronomy, Aarhus University, Ny Munkegade 120, building 1520, 8000 Aarhus C, Denmark.
E-mail address: stefano.alois@phys.au.dk (S. Alois).

http://dx.doi.org/10.1016/j.jaerosci.2016.12.003
Received 15 September 2016; Received in revised form 29 November 2016; Accepted 21 December 2016
Available online 31 December 2016

ionization energy, electron affinity or electro-negativity (Wiles, Grzybowski, Winkleman, & Whitesides, 2003). Despite this some success has been achieved with electron transfer models involving electron donor/acceptors or so called high energy electron states in insulator-insulator contact, also known as a molecular ion state model (Bailey, 2001; Duke & Fabish, 1978; Lowell & Rose-Innes, 1980). Similar electron transfer models also involving so called high energy surface electron states (likely due to impurities/contamination) are used in describing size dependent electrification (Bo, Zhang, Hu, & Zheng, 2013; Harrison et al., 2016; Lacks & Mohan Sankaran, 2011).

Specific electron transfer models have been developed for electrification in metal-insulator contact, for example involving an effective potential difference (Davies, 1969) or performing quantum chemical (electron state) calculations (Shirakawa, Ii, Yoshida, Takashima, Shimosaka & Hidaka, 2010). Models have also studied multiple surface impacts; one involved a capacitance charging model including charge relaxation (electrical discharge) (Matsusyama & Yamamoto, 2006).

Despite these advances in electron transfer models, similar success and progress has also been achieved using ion exchange models specifically involving proton exchange which not only works well for ionic or ion doped materials, but also where water layers may be involved relating to chemical properties such as pH and/or zeta potential (Diaz & Felix-Navarro, 2004; Harper, 1998; Law, Tarnawskyj, Salamida, & Debies, 1995; Mizes, Conwell, & Salamida, 1990), however this has not been demonstrated and is not widely accepted.

In determining (order of magnitude) limits for or expected values of contact electrification there has been considerable success using the ratio of charge/surface area (i.e. the surface charge concentration). In a variety of experimental techniques and over a broad range of grain sizes (μm - mm) the electrification (surface charge concentration) limit has been seen to be of order 0.1 mC/m^2 (or around 600 $e/\mu m^2$) (Lacks & Mohan Sankaran, 2011; Lowell, 1986; Merrison, Jensen, Kinch, Mugford, & Nørnberg, 2004; Nieh & Nguyen, 1988; Poppe, Blum, & Henning, 2000). Many granular electrification studies show significantly lower levels of electrification possibly due to experimental challenges in charge collection (e.g. of order 10^{-3} mC/m^2) e.g. (Gross, Grek, Calle, & Lee, 2001; Sickafoose, Colwell, Horányi, & Robertson, 2001). Also in some studies the contact area is estimated, though in most cases the total particle surface area is used.

So even lacking a detailed physical understanding of the electrification process, there is general agreement on the order of magnitude of the electrification and this is sufficient in most cases to quantify the effect of electrification on, for example, entrainment and transport of sand/dust.

Another common cause for observing reduced electrification in charge collection systems is charge leakage via surface water and therefore related to humidity (Nieh & Nguyen, 1988). Also in dust collection experiments electrostatic aggregation can de-electrify suspended dust, especially when in high concentrations and after long suspension times (Merrison et al., 2012). In relatively recent studies using AFM techniques and well prepared surfaces significantly higher values were reported, though here no account was made for lateral spreading of charge (Horn, Smith, & Grabbe, 1993; McCarty & Whitesides, 2008).

Importantly in many cases electrical breakdown could limit the charge on grains during separation, e.g. dielectric (Paschen) breakdown in air which occurs with voltages above around 300 V and pressure·separation (p·L) values above around 1 mbar·cm. This could provide a quantitative explanation for the experimentally observed upper surface charge concentration and has been supported experimentally in detailed investigation using relatively large polymer micro-spheres (50–500 μm) where the surface charge concentration was seen to be constant and of order 0.1 mC/m^2 (or around 600 $e^-/\mu m^2$) (Logan S. McCarty, Winkleman, & Whitesides, 2007). Also electrical breakdown has been directly observed in some experiments (Harper, 1998; Horn et al., 1993; Matsusaka et al., 2010; McCarty et al., 2007; Tatsushi & Hideo, 1997).

It is widely accepted that particulates of the same composition and of differing size upon contact/separation will have a tendency for larger particulates to electrify positively and smaller ones to electrify negatively. This size dependence has been best demonstrated in laboratory experiments involving sand cascading (Bilici, Toth III, Sankaran, & Lacks, 2014; Forward, Lacks, & Sankaran, 2009; Kok & Lacks, 2009; Lacks, Duff, & Kumar, 2008; Lacks & Levandovsky, 2007; Waitukaitis, Lee, Pierson, Forman, & Jaeger, 2014). However not all experimental studies reproduce this behavior (Kunkel, 1950; Sowinski, Miller, & Mehrani, 2010; Trigwell, Grable, Yurteri, Sharma, & Mazumder, 2003). It should also be noted that in many of these electrification studies multiple particle interactions are involved, including particle-wall interactions, and material purity (surface composition) is not well controlled. A more complex charge exchange behavior can therefore often not be ruled out.

Modelling has been unsuccessful in satisfactorily explaining this size dependence in contact electrification, although several promising models are being pursued. For example one model is based upon electron transfer through so called high energy electron surface states (Apodaca, Wesson, Bishop, Ratner, & Grzybowski, 2010; Bo et al., 2013; Lacks & Mohan Sankaran, 2011). It would be extremely useful here to experimentally identify the precise charge/polarity dependence of contact electrification with grain size, this though has yet to be done.

Techniques involving direct electrical charge extraction are typically ineffective when dealing with dust sized (micrometer) particulates since they are typically well suspended and difficult to extract (e.g. into a Faraday cup). Also they will typically carry less charge and in contact with a surface may not be electrically conductive enough to allow rapid charge extraction. For fine suspended dust other techniques have typically been used to quantify particulate electrification. They rely upon the application of an electric field and the drift of electrified dust grains. The field induced drift velocity can be determined using optical/laser systems to study particle trajectories (mobility) (Kunkel, 1950; Mazumder, Ware, Yokoyama, Rubin, & Kamp, 1991; Merrison et al., 2012) or by extracting dust onto a surface (Merrison et al., 2012). The field induced drift velocity will be proportional to the electrical force and therefore the electrical charge and polarity of the dust grains.

There are several modern experimental techniques which are proving to be extremely informative with regard to contact electrification, one such technique is atomic force microscopy (AFM) (Gady, Reifenberger, & Rimai, 1998; Horn et al., 1993;

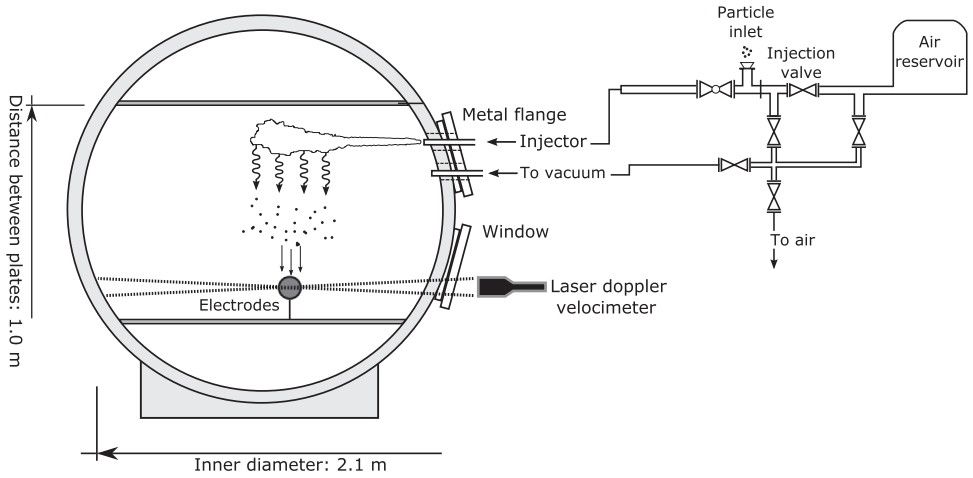

Fig. 1. Schematic of the environmental chamber housing the settling volume and electrodes, the aerosolizer system (upper right) and the Laser Doppler Velocimeter (lower right).

Matsusaka et al., 2010). This work promises to provide a more detailed (atomic scale) understanding of electrification and has already led to the observation that net surface electrification appears to be made up of a 'mosaic' of highly electrified regions of positive and negative patches (Baytekin, Patashinski, Branicki, Baytekin, Soh & Grzybowski, 2011).

2. Materials and methods

The goal of this study is to advance our understanding of contact electrification through a combination of novel experimental techniques applied to aerosol dispersion of micrometer scale particles. Importantly, this study focusses upon fine particles (< 10 μm) relevant to dust suspension and aerosols, unlike many previous experimental studies. Here many physical processes such as adhesion/cohesion or electrical discharging may be extremely sensitive to scale.

Aerosol generation is achieved by the rapid de-compression of a small (~20 cm^3) gas chamber through a tube within which a small mass (typically around 20 mg) of powder has been placed. This gas/particle mixture expands into a large (38 m^3) environmental chamber (Holstein-Rathlou et al., 2014) (Fig. 1). Typically chamber pressures of 2.5–10 mbar and injection pressures of 8.5–40 mbar were used. These pressures were chosen such that the settling velocity was within a measurable range (0.1–5 cm/s). Both capacitance and Pirani type pressure sensors were used for chamber and injection pressure determination (depending on the pressure range) (Holstein-Rathlou et al., 2014). In this pressure range both sensor types have significant inaccuracy and lead to a major source of systematic error in size/charge determination (< 15%).

Typically in this study mono-sized silica (SiO_2) microspheres from Cospheric were used. These particles are extremely spherical and have a narrow size range (see Table 1), they are slightly porous having a mass density of 1.8 g/cm^3. Nominal particle diameters of 1, 2, 4, and 8 μm were used. In specific studies various other morphology and composition of particle were used (see Table 1) as well as other composition of injector tube (specifically glass and quartz).

In one of the measurement techniques used here the aerosol cloud was allowed to settle through a pair of parallel electrodes

Table 1
Simultaneous measurements of size and particle electrification for various combinations of particle composition, particle size (range) and injector tube composition. For the size the mean and standard deviation are generally given both as quoted by the manufacturer and as measured. For the charge per particle (Q) and charge per surface area ($Q/4\pi r^2$) the median value is given as well as the first and third quartiles (in brackets) rather than the standard deviation since typically these distributions are not symmetrical. Note also that these are not the error on the determination of the median value (standard error which typically was between 1–10%), but rather an expression of the width of the distribution of determined values.

Particle type	Injector material	Nominal d [μm]	Measured d [μm]	Q $[10^3 \cdot e^-]$	$Q/4\pi r^2$ $[e^-/\mu m^2]$
Silica 1 μm	Steel	1.18 (0.03)	1.45 (0.45)	−0.4 (+0.2 −0.3)	−70 (+12 −25)
Silica 2 μm	Steel	1.86 (0.06)	1.99 (0.37)	−1.4 (+0.5 −0.7)	−124 (+44 −41)
Silica 4 μm	Steel	3.62 (0.2)	3.95 (0.35)	−4.0 (+1.2 −1.3)	−85 (+30 −34)
Silica 8 μm	Steel	7.75 (0.3)	8.31 (0.55)	−15.6 (+7.4 −6.5)	−77 (+40 −27)
Soda lime glass	Steel[b]	1–8	2.38 (1.68)	−1.1 (+0.5 −0.8)	−107 (+42 −20)
Copper	Glass[b]	< 5	5.32 (3.85)	+6.5 (+14.7 −3.6)	+127 (+120 −54)
Tungsten[a]	Glass[b]	1–5	7.85 (5.07)	−9.7 (+7.3 −19.5)	−86 (+33 −36)
Al Oxide[a]	Quartz	5 (mean)	4.96 (1.47)	+3.5 (+5.0 −2.7)	+39 (+103 −29)

[a] The samples are not spherical.
[b] Injected from the top of the environmental chamber.

across which an alternating electric field was applied (Kunkel, 1950). A two dimensional Laser Doppler Velocimeter (Dantec LDV) was then used to (instantaneously) measure the horizontal and vertical velocity of an individual aerosol particle. The LDV measurement volume was around 1.3 mm^3.

Assuming the particles are spherical the measured horizontal (U_E) and vertical (U_g) velocities can be used to derive the respective electrical charge (Q) and radius (r). Typically, given the particle size and gas density, drag is described by molecular scattering (within the molecular drag regime) as characterized by a Knudsen number greater than 1 ($Kn = \lambda/2r > 1$), where λ is the mean free path or scattering length ($\lambda = \frac{\mu}{\rho_f}\sqrt{\frac{\pi}{2}\frac{m_{mol}}{KT}}$) (Epstein, 1924)

$$r = \frac{U_g \delta \rho_f}{g \rho_p} \sqrt{\frac{3KT}{m_{mol}}} \tag{1}$$

$$Q = \frac{4\pi\delta\rho_f r^2 U_E}{3E} \sqrt{\frac{3KT}{m_{mol}}} \tag{2}$$

Where μ is the molecular viscosity of the gas, ρ_f is its density, m_{mol} is its molecular mass, K is the Boltzmann constant, T is the temperature (around 300 K), E is the electric field and ρ_p is the particle mass density and g is the gravitational acceleration. In this experiment the free parameter in Epstein's drag model has been taken as $\delta = 1.15$, based on a previous (unpublished) study of settling speeds (personal communication, Jakobsen 2016).

The vertical electrodes used had a separation = 2.2 cm and diameter = 5 cm and voltages of 15–600 V were used corresponding to electric fields in the range $7{\cdot}10^2$–$2.7{\cdot}10^4$ V/m. An alternating electric field was used with frequency around 10 Hz in order to avoid drift of the electrified particles out of the measurement volume. Note that for micron sized particles (even in low density gas) particles rapidly reach terminal velocity within the chamber (typically the particle characteristic time $\tau < 10^{-2}$ ms). Particles counted within a time $< \tau$ with respect to the polarity-switch time were deleted from the results to ensure the terminal velocity to be reached.

Typically the aerosol injector was orientated horizontally and around 1 m from and 0.6 m above the electrodes (LDV detection volume, see Fig. 1), however it was also possible to inject from the top of the chamber. A micrometer driven system was used to control the orientation of the jet with respect to the measurement volume such that the electrification of different sections of the jet structure could be sampled.

In a second measurement technique, the voltage (V) generated on the stainless steel injection tube was measured using an oscilloscope (Tektronix DPO 2002B) attached to the electrically isolated injector tube (V). Knowing the impedance of the oscilloscope probe (R = 10 MΩ) the net electrical current leaving the injection (aerosolizing) nozzle can be determined as a function of time; $dQ/dt = V(t)/R$. By integration the total electrical charge leaving the (conductive) injector system can then be obtained. Note that the injector system will be functioning here as a Faraday cage and will therefore only be sensitive to electrical charge exiting/entering the injector system. The oscilloscope ground was attached to the (metal) environmental chamber and a second oscilloscope probe was used to monitor possible electrical charges entering from the gas injection side.

A high speed camera (Edgertronics) was used within the environmental chamber in order to study the spatial and temporal structure of the aerosol jet/plume. It could also be used to correlate the observed (time dependent) particle flux with the measured electrical current leaving the nozzle.

In the case of insulating injector tubes the injector system was externally coated in conductive material (a Faraday cage).

3. Results

The aerosol spatial structure was seen to consist of an inner, highly concentrated central jet and a more diffuse and divergent outer vortex ring. By controlling the injector direction with respect to the LDV/electrode system these different components could be studied individually. This can be seen in Fig. 2 showing that the outer particles are (relatively) highly electrified whereas those in the central jet have low electrification per particle. In some cases it was difficult to isolate the individual components (see Fig. 3).

Remarkably, when looking only at the outer highly electrified particles, it is seen that they are all electrified negatively and have a similar and size independent surface charge concentration (Fig. 3. and Fig. 4). That is to say that the electrical charge per particle appears to be constant for a given grain size and increases with r^2 (i.e. surface area). This value is seen to be around -100 $e^-/\mu m^2$ (or around -0.02 mC/m^2) if assumed to be uniform over the entire particle surface.

Although a maximum electrification per particle was expected from previous studies, for the μm scale particles to attain such a narrow range of particle electrification was unexpected. The charge/grain of around 500 – 30000 e^- is in reasonable agreement with previous studies e.g. (Merrison et al., 2012) also this charge/surface area is below the expected maximum of around 0.1 mC/m^2. The results here typically consisted of several repeated aerosol injections per particle type/injection condition with 20–700 counts per injection. For the finer particles (e.g. 1 μm diameter) it was often observed that doubly electrified grains were also seen (see Fig. 4), this was probably due to an aggregated pair of particles, an effect which was also seen in the size distribution (Fig. 5).

In order to verify that these electrification effects were not peculiar to the use of this combination of a steel tube and silica microspheres, other tube/powder material combinations have been tested. This has included; Soda Lime glass spheres in steel, Tungsten in borosilicate glass, Aluminium oxide in Quartz and Copper in borosilicate glass. Interestingly for Aluminium Oxide and Copper the particles are seen to become positively electrified, however for all particle types the magnitude of the charge per surface area appears to be similar i.e. the same order of magnitude (see Fig. 6 and Table 1).

The jet structure, aerosol concentration (dispersion) and average electrification are all sensitive to injection geometry and

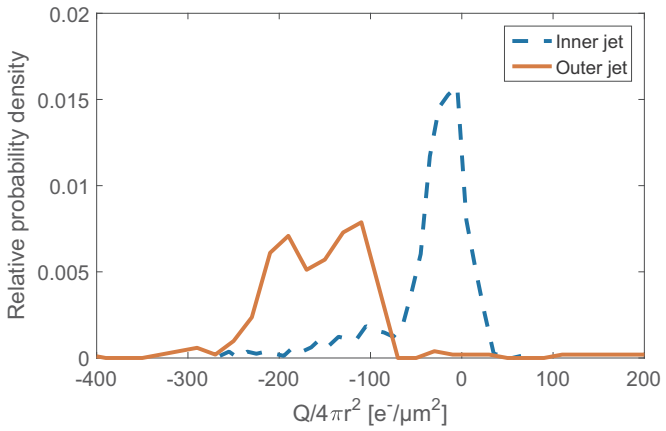

Fig. 2. Electrification per surface area determined for aerosolized particles (2 μm silica microspheres) within the inner portion of the jet (blue dashed line) and separately particles within the outer portion of the jet (red line). These different portions were isolated by careful manipulation of the injector tube orientation with respect to the measurement volume (electrodes). (For interpretation of the references to color in this figure legend, the reader is referred to the web version of this article.)

pressure. When using the LDV measurement technique relatively low injection pressures and low chamber pressures (< 20 mbar) were required in order to obtain sufficiently high terminal velocities. In the case of injection at low over pressure many of the particles were not dispersed and either remained within the injector tube or were injected as aggregates which were observed to be as large as mm size. Evidence has been seen for the build-up of microspheres within the injector tube, specifically: reduced particle dispersion after cleaning of the injector, aerosol generation even without adding further powder material, and also evidence for electrical breakdown after repeated injections.

In Fig. 7 the voltage generated on the injection tube is shown together with an analysis of the high speed camera observations whereby the light intensity is quantified as a function of time within a small (400 mm^3) volume just outside of the nozzle. In this time sequence one can see that the net electrical flux leaving the tube is correlated with the observable particle flux, but is variable in time. In addition, some of the peaks in injector voltage are associated with (mm size) aggregates leaving the tube (and are therefore assumed to be highly electrified) while others show no detectable variation in injector voltage. The charge associated with such aggregates was determined to be as high as e.g. Q ~ $-1.5{\cdot}10^8$ e^-. An estimate of the aggregate size (diameter around 1 mm) was found from high speed video images giving calculation of its charge per surface area, assuming it is spherical, a value of ~ 55 $e^-/\mu m^2$, presumably coincidentally this is a similar value with respect to the single particles surface charge concentration. In this injection the over pressure was around 22 mbar into a chamber pressure of around 13 mbar. The effective surface voltage of the aggregate in this case would be around ~ 400 V which is in reasonable agreement with that expected if limited by gas breakdown at this pressure-distance range (~ 1 mbar cm).

In some cases (though not always) evidence for multiple electrical discharges were observed, this was characterized by extremely rapid (1 ns) and intense (> 1 V) spikes seen on the injector voltage (Fig. 8). Although no observable electrical discharges were seen at the nozzle (with the high speed camera) it is likely that this was the site for the discharges. Alternatively electrical discharges could

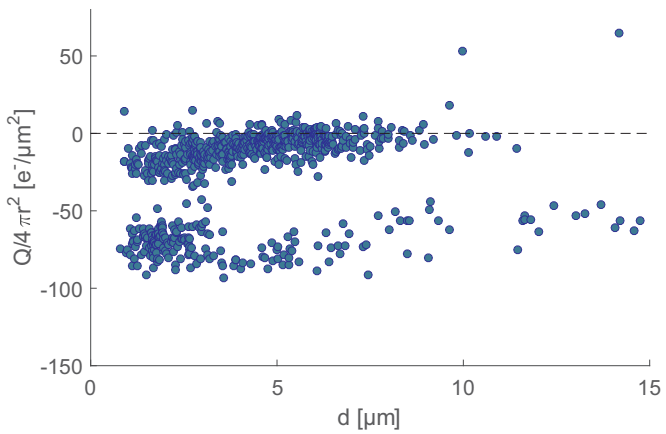

Fig. 3. Individual measurements of particle size (diameter d) and determination of electrification per surface area for a single injection (aerosolization) of Soda Lime glass micro-spheres (1–8 μm, see Table 1). In this injection, both inner (relatively low electrification) and outer (relatively highly electrified) portions of the jet were observed again by careful manipulation of the injector tube orientation with respect to the measurement volume (electrodes) which in this case was placed above the electrode system (injected from the top of the environmental chamber).

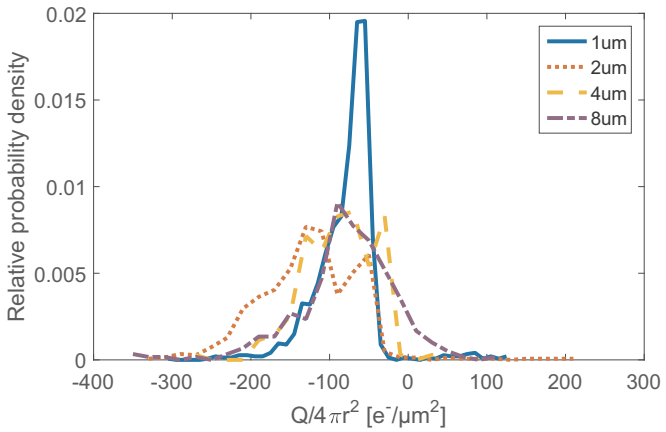

Fig. 4. Compiled results for determination of the surface charge concentration ($Q/4\pi r^2$) for various sized silica micro-spheres (1, 2, 4 and 8 μm). Although the distributions do have a significant width and include some fraction of relatively low electrification, they seem share a central high concentration with a value around 100 $e^-/\mu m^2$.

in principle generate ions such that an electrical pulse of this type would be observed. However, the particle Stokes number during the injection process can be seen to be $St = \tau U_0/D_i < 1$ (with U_0 the flow velocity, D_i the injector diameter) for the conditions used here, indicating that single microspheres should not be separated from the gas flow.

The dependence of these electrification (and discharging) effects on gas composition was investigated using the gases Argon and CO_2 in addition to air. These gases have differing minimum electrical breakdown voltages (of respectively around 140, 460, 330 V) however no significant variation in electrification or discharging was observed using these various gases.

4. Discussion

The primary goal of this study was to investigate (quantify) the contact electrification process using novel, precision techniques and advanced micro-particles (spherical and mono-sized). Specifically the particle size dependence of the process was to be studied. Surprisingly the particles interacting with the injector tube were seen to obtain a certain (narrowly distributed) quantity of negative charge which increased with particle surface area, giving a relatively constant observed surface concentration of around -100 $e^-/\mu m^2$ (or 0.02 mC/m^2) (see Fig. 4). How these observations can be explained within current models of contact/tribo-electrification will be discussed.

Firstly the concept of a maximum surface charge concentration is well known and is supported by a broad range of experiments (Lacks & Mohan Sankaran, 2011; Lowell, 1986; Merrison et al., 2004; Nieh & Nguyen, 1988; Poppe et al., 2000) with values expected to be around 0.1 mC/m^2. However a large set of close to identically electrified micron scale particles (with apparently constant surface charge concentration) has not been suggested previously.

Clearly in these experiments multiple collisions and many body effects may occur, however it is not clear that this would in itself

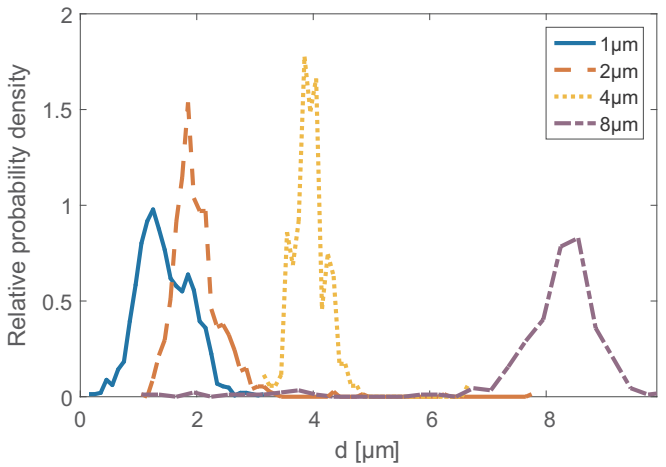

Fig. 5. Measurements of silica microsphere diameter (using the LDV technique) for the four different nominal sizes of 1, 2, 4 and 8 μm (respectively shown as; blue solid, red dashed, yellow dotted and purple dash-dot lines). (For interpretation of the references to color in this figure legend, the reader is referred to the web version of this article.)

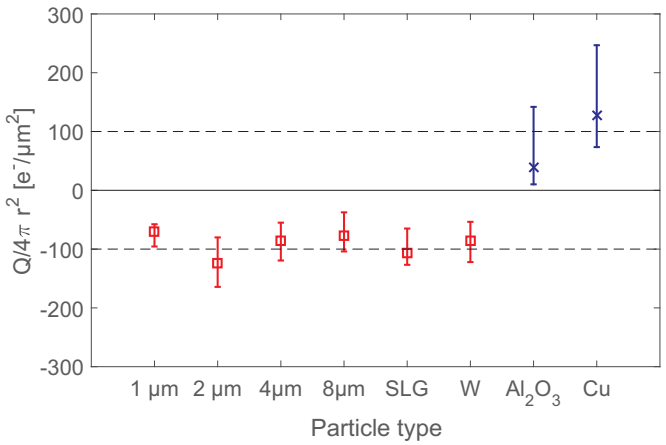

Fig. 6. Simultaneous measurements of size and particle electrification for various combinations of particle composition, particle size (range) and injector tube composition. Particle type/injector tube type the nominal description is used, for more information see also Table 1. For the charge per surface area ($Q/4\pi r^2$) the median value is given with the error bars denoting the first and third quartiles (i.e. spanning 50% of the distribution) rather than the standard deviation since typically these distributions are not symmetrical. Note also that these are not the error on the determination of the median value (i.e. standard error which typically was between 1–10%), but rather an expression of the width of the distribution of determined values.

lead to the observed well defined class of uniformly electrified particles. Rather the injection process is observed to be essentially turbulent with strong temporal and spatial variation in particle concentration and flow velocity, this might be expected lead to a broad distribution of electrification states.

A possible explanation compatible with previous work would be a high degree of initial contact electrification combined with the concept of a maximum charge concentration leading to essentially all of the particles attaining the same surface charge. The nature of this limiting process might be electrical break down. However the surface voltage of these (e.g. 1 μm) microspheres can be calculated to be only around 2 V which is well below the minimum gas breakdown voltage (of > 300 V) also the scale of the particles and gas pressure used here should make this process extremely unlikely (pressure·diameter < 0.01 mbar·cm) given the Paschen curve for air.

Although gas discharge is not expected for single micro-particles, at the macroscopic scale of the injection tube, i.e. around 1mm, this could explain the occasionally observed electrical discharges (see Fig. 6.) and might also limit the electrification of particle aggregates. The minimum Paschen breakdown voltage for air is around 300 V and is expected at a value of pressure·diameter of around 1 mbar·cm. For an electrified particle concentration of order $10^4/mm^3$ (which is not unreasonable given the potential number of particles per injection e.g. $> 10^8$) this would generate a voltage of order 100 V between the particles and the injector tube and at a value of p·L close to the minimum for Paschen breakdown. Electrified aggregates were observed with a charge of up to $Q \sim 1.5 \cdot 10^8 e^-$, this is also seen to be compatible with the gas discharge limitation i.e. a surface potential of several hundred Volts at a p·L of around 1 mbar·cm.

Many contact electrification processes (both electron and ion transfer) involve modelling of the contact area and charge exchange

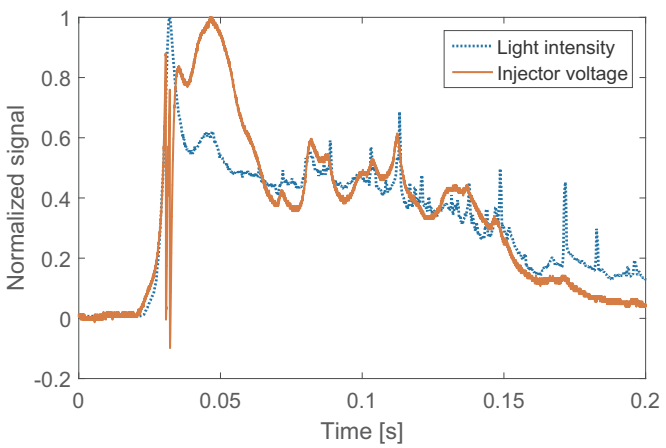

Fig. 7. The blue dotted line shows the light intensity observed using a high speed camera quantified as a function of time within a small (400 mm^3) volume just outside of the aerosol injector nozzle. The red line shows the corresponding voltage measured on the injector tube. In this time sequence one can see that the net electrical flux leaving the tube is correlated with the observable particle flux. In addition, some of the peaks in injector voltage are associated with observable (up to mm size) aggregates leaving the tube (and are therefore assumed to be highly electrified) while others show no detectable variation in injector voltage. (For interpretation of the references to color in this figure legend, the reader is referred to the web version of this article.)

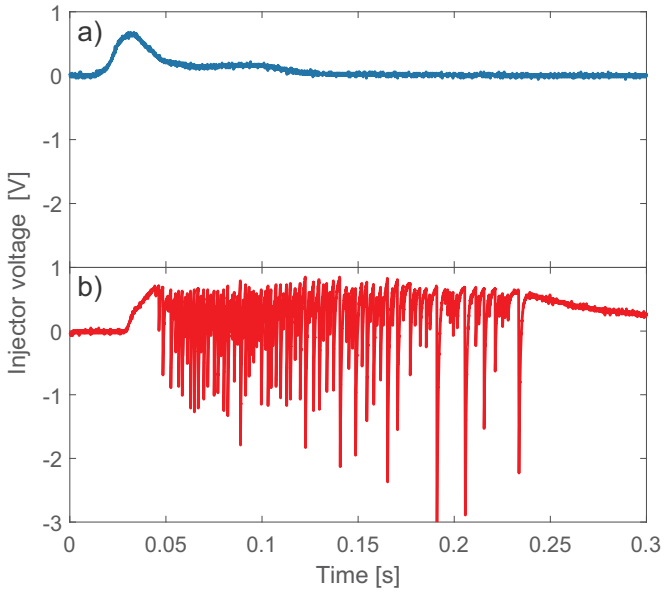

Fig. 8. Voltage measured on the injection tube during an aerosolizing injection, it should correspond to the rate of charge leaving (or entering) the system. a) shows the first injection after cleaning of the injection system, b) shows an injection performed after repeated injections in which it is assumed that accumulation of particulates has occurred leading to increased charge exchange and also the observation of numerous "discharge" like features, these have a rapid onset (fall lasting of the order of 1 ns) and an exponential return to previous voltage. The rapid onset is assumed to be a sudden transfer of charge between the electrified aerosol and the injector tube within the chamber. The exponential decay is compatible the subsequent discharge of the injector tube through the oscilloscope probe resistor (10 MΩ).

increasing with this area (McCarty & Whitesides, 2008). The radius of the contact surface can be estimated as $a = (3Fr/4E_*)^{1/3}$ following the Hertzian model (Thornton & Ning, 1998), with r the particle radius, F = 30 nN the adhesive force (Jones, Pollock, Geldart, & Verlinden-Luts, 2004), and E_* is the effective Young's modulus (40 GPa). This gives a contact surface area $\pi a^2 \sim 400nm^2$. Assuming the measured charge to be concentrated in this contact area would give $\sim 3{\cdot}10^7$ $e^-/\mu m^2$ and would lead to an electric field on separation of around $E \sim 3{\cdot}10^{11}$ V/m. This ignores processes such as lateral charge spreading and roughness of the surfaces which might increase the effective contact area. Electron field emission is expected for electric fields exceeding $E > 10^9$ V/m e.g. (Harper, 1998; McCarty & Whitesides, 2008). Hence an alternative process for limiting particle electrification could be field emission at the contact site.

This seems to be the most likely explanation, however if electrical discharging is not the cause of the observed narrow range of single-particle surface electrification then presumably the cause must lie in the charge generation process itself.

It should also be noted that the surfaces used here are not well prepared (on a molecular level), it would therefore be somewhat surprising if relatively well defined surface charge is generated since the condition of individual contact sites would be expected to vary in physical/chemical condition (Baytekin et al., 2011).

Many Ion exchange models of contact electrification involve the presence of surface water layers (water bridging) which might be less sensitive to specific properties of the contact site. Although humidity is difficult to eliminate entirely, given the low pressure (and often dry gas) conditions employed in these experiments this would not be considered a humid environment (typically RH < 2%).

It is generally accepted (based upon previous observations) that in particle-particle interaction smaller particles electrify more negatively. Based upon this expected size dependence of contact electrification (Lacks & Levandovsky, 2007; Waitukaitis et al., 2014) one would expect that the larger particles would have a tendency to become less negatively (more positively) electrified, which is not consistent with these observations.

5. Conclusions

In this study novel precision techniques have been applied in order to study the contact electrification process in solid (powder) aerosol generation. One laser based technique involves the simultaneous determination of size and electrical charge of individual particles within the aerosol. Surprisingly when interacting with the injector tube silica microspheres were found to attain a relatively narrow range of surface charge concentration centered around -100 $e^-/\mu m^2$ (or around 0.02 mC/m^2) irrespective of size (in the range 1–8 μm). Although this value is in reasonable agreement with the maximum expected electrification estimated from previous experimental studies (< 0.1 mC/m^2), its cause is not obvious from conventional models.

Several combinations of aerosol particle and injector tube composition were investigated, some of which led to positive particle electrification and all of which resulted in similar values of measured surface charge concentration.

Various models for this electrification process have been considered here, including ion and electron transfer processes, size dependent electrification and electrical breakdown. Although a definitive model has not been demonstrated, the most likely

explanation for the observed uniform surface electrification seems to be that the contact electrification transfers in excess of the observed charge and that a combination of field emission and possibly charge spreading occur as the particle leaves the surface which then reduces the charge concentration to a specific observed value (for each particle).

Despite the persistent lack of a general model for contact electrification, experimentally determined values such as those presented here are of considerable use in predicting and understanding electrification in aerosol generation and transport as well as placing further requirements to possible models.

In the future these techniques could be usefully applied to study the material dependence of contact electrification and also the particle-particle size dependence. Note also that the temperature and humidity dependence of contact electrification would be interesting and potentially useful to study in the future.

Acknowledgements

We would like to thank Andreas Boes Jakobsen for his valuable input. Thanks also to Ulrich Kueppers and the rest of the VERTIGO team for their support. This work is supported by the Marie Curie Initial Training Network 'VERTIGO', funded through the European Seventh Framework Programme (FP7 2007–2013) under Grant Agreement number 607905. This laboratory is a member of Europlanet 2020 RI which has received funding from the European Union's Horizon 2020 research and innovation programme under grant agreement No 654208.

References

Apodaca, M. M., Wesson, P. J., Bishop, K. J., Ratner, M. A., & Grzybowski, B. A. (2010). Contact electrification between identical materials. *Angewandte Chemie*, 122(5), 958–961.

Bailey, A. G. (2001). The charging of insulator surfaces. *Journal of Electrostatics*, 51, 82–90.

Baytekin, H., Patashinski, A., Branicki, M., Baytekin, B., Soh, S., & Grzybowski, B. A. (2011). The mosaic of surface charge in contact electrification. *Science*, 333(6040), 308–312.

Bilici, M. A., Toth, J. R., III, Sankaran, R. M., & Lacks, D. J. (2014). Particle size effects in particle-particle triboelectric charging studied with an integrated fluidized bed and electrostatic separator system. *Review of Scientific Instruments*, 85(10), 103903.

Bo, T.-L., Zhang, H., Hu, W.-W., & Zheng, X.-J. (2013). The analysis of electrification in windblown sand. *Aeolian Research*, 11, 15–21.

Davies, D. (1969). Charge generation on dielectric surfaces. *Journal of Physics D: Applied Physics*, 2(11), 1533.

Diaz, A. F., & Felix-Navarro, R. M. (2004). A semi-quantitative tribo-electric series for polymeric materials: The influence of chemical structure and properties. *Journal of Electrostatics*, 62(4), 277–290http://dx.doi.org/10.1016/j.elstat.2004.05.005.

Duke, C., & Fabish, T. (1978). Contact electrification of polymers: A quantitative model. *Journal of Applied Physics*, 49(1), 315–321.

Epstein, P. S. (1924). On the resistance experienced by spheres in their motion through gases. *Physical Review*, 23(6), 710.

Forward, K. M., Lacks, D. J., & Sankaran, R. M. (2009). Charge segregation depends on particle size in triboelectrically charged granular materials. *Physical Review Letters*, 102(2), 028001. http://dx.doi.org/10.1103/PhysRevLett.102.028001.

Gady, B., Reifenberger, R., & Rimai, D. S. (1998). Contact electrification studies using atomic force microscope techniques. *Journal of Applied Physics*, 84(1), 319. http://dx.doi.org/10.1063/1.368078.

Gross, F. B., Grek, S. B., Calle, C. I., & Lee, R. U. (2001). JSC Mars-1 Martian Regolith simulant particle charging experiments in a low pressure environment. *Journal of Electrostatics*, 53(4), 257–266.

Harper, W. R. (1998). *Contact and frictional electrification* Morgan Hill, Calif: Laplacian Press.

Harrison, R. G., Barth, E., Esposito, F., Merrison, J., Montmessin, F., Aplin, K., & Farrell, W. M. (2016). Applications of electrified dust and dust devil electrodynamics to Martian atmospheric electricity. *Space Science Reviews*, 1–47.

Holstein-Rathlou, C., Merrison, J., Iversen, J. J., Jakobsen, A. B., Nicolajsen, R., Nørnberg, P., & Portyankina, G. (2014). An environmental wind tunnel facility for testing meteorological sensor systems. *Journal of Atmospheric and Oceanic Technology*, 31(2), 447–457. http://dx.doi.org/10.1175/jtech-d-13-00141.1.

Horn, R. G., Smith, D., & Grabbe, A. (1993). Contact electrification induced by monolayer modification of a surface and relation to acid-base interactions. *Nature*, 366, 442–443.

James, M. R., Wilson, L., Lane, S. J., Gilbert, J. S., Mather, T. A., Harrison, R. G., & Martin, R. S. (2008). Electrical charging of volcanic plumes. *Space Science Reviews*, 137(1-4), 399–418. http://dx.doi.org/10.1007/s11214-008-9362-z.

Jones, R., Pollock, H. M., Geldart, D., & Verlinden-Luts, A. (2004). Frictional forces between cohesive powder particles studied by AFM. *Ultramicroscopy*, 100(1), 59–78.

Karner, S., & Anne Urbanetz, N. (2011). The impact of electrostatic charge in pharmaceutical powders with specific focus on inhalation-powders. *Journal of Aerosol Science*, 42(6), 428–445. http://dx.doi.org/10.1016/j.jaerosci.2011.02.010.

Kok, J. F., & Lacks, D. J. (2009). Electrification of granular systems of identical insulators. *Physical Review E*, 79(5), 051304.

Kunkel, W. B. (1950). The static electrification of dust particles on dispersion into a cloud. *Journal of Applied Physics*, 21(8), 820. http://dx.doi.org/10.1063/1.1699765.

Lacks, D. J., Duff, N., & Kumar, S. K. (2008). Nonequilibrium accumulation of surface species and triboelectric charging in single component particulate systems. *Physical Review Letters*, 100(18), 188305.

Lacks, D. J., & Levandovsky, A. (2007). Effect of particle size distribution on the polarity of triboelectric charging in granular insulator systems. *Journal of Electrostatics*, 65(2), 107–112. http://dx.doi.org/10.1016/j.elstat.2006.07.010.

Lacks, D. J., & Mohan Sankaran, R. (2011). Contact electrification of insulating materials. *Journal of Physics D: Applied Physics*, 44(45), 453001. http://dx.doi.org/10.1088/0022-3727/44/45/453001.

Law, K.-Y., Tarnawskyj, I. W., Salamida, D., & Debies, T. (1995). Investigation of the contact charging mechanism between an organic salt doped polymer surface and polymer-coated metal beads. *Chemistry of Materials*, 7(11), 2090–2095.

Lowell, J. (1986). Constraints on contact charging of insulators. I. Spatial localisation of insulator states. *Journal of Physics D: Applied Physics*, 19(1), 95.

Lowell, J., & Rose-Innes, A. (1980). Contact electrification. *Advances in Physics*, 29(6), 947–1023.

Matsusaka, S., Maruyama, H., Matsuyama, T., & Ghadiri, M. (2010). Triboelectric charging of powders: A review. *Chemical Engineering Science*, 65(22), 5781–5807. http://dx.doi.org/10.1016/j.ces.2010.07.005.

Matsusyama, T., & Yamamoto, H. (2006). Impact charging of particulate materials. *Chemical Engineering Science*, 61(7), 2230–2238. http://dx.doi.org/10.1016/j.ces.2005.05.003.

Mazumder, M., Ware, R., Yokoyama, T., Rubin, B., & Kamp, D. (1991). Measurement of particle size and electrostatic charge distributions on toners using E-SPART analyzer. *IEEE Transactions on Industry Applications*, 27(4), 611–619.

McCarty, L. S., & Whitesides, G. M. (2008). Electrostatic charging due to separation of ions at interfaces: Contact electrification of ionic electrets. *Angewandte Chemie International Edition*, 47(12), 2188–2207. http://dx.doi.org/10.1002/anie.200701812.

McCarty, L. S., Winkleman, A., & Whitesides, G. M. (2007). Ionic electrets: Electrostatic charging of surfaces by transferring mobile ions upon contact. *Journal of the American Chemical Society*, 129(13), 4075–4088. http://dx.doi.org/10.1021/ja067301e.
Merrison, J. (2012). Sand transport, erosion and granular electrification. *Aeolian Research*, 4, 1–16.
Merrison, J., Jensen, J., Kinch, K., Mugford, R., & Nørnberg, P. (2004). The electrical properties of Mars analogue dust. *Planetary and Space Science*, 52(4), 279–290.
Merrison, J. P., Gunnlaugsson, H. P., Hogg, M., Jensen, M., Lykke, J., Madsen, M. B., & Pedersen, R. (2012). Factors affecting the electrification of wind-driven dust studied with laboratory simulations. *Planetary and Space Science*, 60(1), 328–335.
Mizes, H., Conwell, E., & Salamida, D. (1990). Direct observation of ion transfer in contact charging between a metal and a polymer. *Applied physics letters*, 56(16), 1597–1599.
Nieh, S., & Nguyen, T. (1988). Effects of humidity, conveying velocity, and particle size on electrostatic charges of glass beads in a gaseous suspension flow. *Journal of Electrostatics*, 21(1), 99–114.
Poppe, T., Blum, J., & Henning, T. (2000). Experiments on collisional grain charging of micron-sized preplanetary dust. *The Astrophysical Journal*, 533(1), 472.
Shirakawa, Y., Ii, N., Yoshida, M., Takashima, R., Shimosaka, A., & Hidaka, J. (2010). Quantum chemical calculation of electron transfer at metal/polymer interfaces. *Advanced Powder Technology*, 21(4), 500–505.
Sickafoose, A., Colwell, J., Horányi, M., & Robertson, S. (2001). Experimental investigations on photoelectric and triboelectric charging of dust. *Journal of Geophysical Research: Space Physics*, 106(A5), 8343–8356.
Sowinski, A., Miller, L., & Mehrani, P. (2010). Investigation of electrostatic charge distribution in gas–solid fluidized beds. *Chemical Engineering Science*, 65(9), 2771–2781.
Tanoue, K.-i, Ema, A., & Masuda, H. (1999). Effect of material transfer and work hardening of metal surface on the current generated by impact of particles. *Journal of Chemical Engineering of Japan*, 32(4), 544–548.
Tatsushi, M., & Hideo, Y. (1997). Charge-relaxation process dominates contact charging of a particle in atmospheric condition: II. The general model. *Journal of Physics D: Applied Physics*, 30(15), 2170.
Thornton, C., & Ning, Z. (1998). A theoretical model for the stick/bounce behaviour of adhesive, elastic-plastic spheres. *Powder Technology*, 99(2), 154–162http://dx.doi.org/10.1016/S0032-5910.
Trigwell, S., Grable, N., Yurteri, C. U., Sharma, R., & Mazumder, M. K. (2003). Effects of surface properties on the tribocharging characteristics of polymer powder as applied to industrial processes. *IEEE Transactions on Industry Applications*, 39(1), 79–86.
Waitukaitis, S. R., Lee, V., Pierson, J. M., Forman, S. L., & Jaeger, H. M. (2014). Size-dependent same-material tribocharging in insulating grains. *Physical Review Letters*, 112(21), 218001.
Wiles, J. A., Grzybowski, B. A., Winkleman, A., & Whitesides, G. M. (2003). A tool for studying contact electrification in systems comprising metals and insulating polymers. *Analytical Chemistry*, 75(18), 4859–4867.